

Comparison of A-block polydispersity effects on BAB triblock and AB diblock copolymer melts

M.W. Matsen^a

School of Mathematical and Physical Sciences, University of Reading, Whiteknights, Reading RG6 6AX, UK

Received 14 February 2013 and Received in final form 31 March 2013

Published online: 25 April 2013 – © EDP Sciences / Società Italiana di Fisica / Springer-Verlag 2013

Abstract. Recent experiments on triblock copolymer melts suggest that polydispersity effects are dramatically enhanced when polydisperse blocks are constrained by both ends to the internal interfaces of an ordered morphology. To quantify the relevance of architecture, we compare BAB triblock and AB diblock copolymer melts with polydisperse A blocks and monodisperse B blocks, using self-consistent field theory (SCFT). We do, in fact, find an enhanced shift in the order-order transitions (OOTs) of the triblock copolymer system in good agreement with the experiments, which we attribute to a reduction of entropy in the A-rich domains due to the absence of chain ends. There is also a slightly enhanced dilation of the domains, but not nearly to the same degree as reported by the experiments. Unlike in the experiments, our calculations indicate that the polydispersity-induced shifts in the order-disorder transition (ODT) should be quantitatively similar for both diblocks and triblocks. It is possible that some of the pronounced effects observed in the experiments have more to do with the detailed shape of the molecular-weight distribution than the triblock architecture.

1 Introduction

Block copolymers continue to receive considerable attention because of numerous applications relating to their ability to form ordered morphologies with nano-sized domains. However, development is often impeded by the high cost of production and the limited range of potential chemistries due to a perceived need for anionic polymerization, because of a long-held opinion that the formation of well-ordered morphologies requires low levels of polydispersity [1, 2]. Fortunately, experimentalists have begun to realize that this is not necessarily the case [1–3], implying that it may be acceptable to synthesize block copolymers via less costly methods. This has, in turn, inspired efforts to better understand how the phase behavior of block copolymer melts is affected by elevated degrees of polydispersity. The model system for most of the experimental work [4–8] has been AB diblock copolymers with polydisperse A blocks and monodisperse B blocks.

The experiments have found that polydispersity increases the domain size, D , and shifts the order-order transitions (OOTs) towards larger volume fractions, f_A , of the polydisperse domains. These effects are well accounted for by theory [9–11] and are easily understood. The behavior originates from the fact that polydispersity reduces the entropic stretching energy required to increase the thickness of a polymer brush [12]. Figure 1 provides the simple

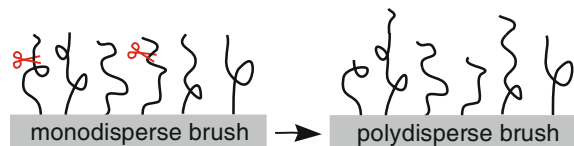


Fig. 1. Monodisperse brushes can be transformed into polydisperse brushes by snipping fragments off some polymer chains and joining them to other chains. This increases the average brush thickness without any additional stretching of the chains.

intuitive explanation; monodisperse brushes can be transformed in polydisperse brushes by cutting the ends off some chains and adding them to other chains, which increases the average brush thickness without any additional stretching of the chains. In an ordered block-copolymer morphology, this reduction in the cost of stretching polydisperse (A-rich) domains leads to the dilation of the domains. The monodisperse (B-rich) domains are also able to reduce their stretching energy by curving the internal interfaces towards the polydisperse domains, which causes the shift in the OOTs.

Polydispersity also alters the location of the order-disorder transition, $(\chi N)_{\text{ODT}}$, where N refers to the number-averaged polymerization index and χ is the usual Flory-Huggins interaction parameter. Evidently, there are two competing effects [13, 14]. On one hand, the presence of the higher molecular-weight molecules helps induce microphase separation, which pushes $(\chi N)_{\text{ODT}}$ to

^a e-mail: m.w.matsen@reading.ac.uk

smaller values. On the other hand, polydispersity relieves the high levels of packing frustration in disordered morphologies, which increases $(\chi N)_{\text{ODT}}$. The net result is that $(\chi N)_{\text{ODT}}$ decreases when the polydisperse blocks form the minority component (*i.e.*, $f_A \lesssim 0.5$), and it increases when the polydisperse blocks are the majority component (*i.e.*, $f_A \gtrsim 0.5$) [6]. Mean-field theory misses the second effect because it treats the disordered phase as a homogeneous mixture of A and B segments rather than a fluctuating morphology of irregularly shaped domains, and thus it incorrectly predicts a decrease in $(\chi N)_{\text{ODT}}$ at all compositions [9, 11, 15]. As one might expect, the correct behavior is captured by Monte Carlo simulations [13, 14].

Now that the diblock system is reasonably well understood, researchers are beginning to explore more elaborate architectures. Interestingly, studies from the group of Mahanthappa [16–18] have reported unexpectedly large polydispersity effects for melts of BAB triblock copolymer in comparison to AB diblock copolymers, when the A block is polydisperse. For middle-block polydispersities approaching $\text{PDI}_A = 2$, non-lamellar phases appear at symmetric compositions, domain sizes increase by a factor of around two, and $(\chi N)_{\text{ODT}}$ decreases by a factor of about two. This seems to contradict the principle that symmetric triblocks should behave equivalently to the homologous diblocks formed by snipping all the triblocks in half [19]. Here we use the numerical self-consistent field theory (SCFT) of Helfand [20] to examine the degree to which architecture is responsible for these pronounced effects by comparing melts of polydisperse triblock copolymer with their homologous diblock counterpart. We also examine the strong-segregation theory (SST) of Semenov [21], which provides analytical predictions corresponding to the exact $\chi N \rightarrow \infty$ limit of SCFT [22].

2 Results

Self-consistent field theory is a well-documented method [23, 24], and so we forgo a detailed description of the calculation. It is sufficient to say that we perform the SCFT on the standard Gaussian chain model [25] in the canonical ensemble using the usual Schulz-Zimm distribution [26, 27],

$$p(\sigma) = \frac{k^k \sigma^{k-1} \exp(-k\sigma)}{\Gamma(k)}, \quad (1)$$

where $\sigma = N_A/(N_A)_n$ is the size of an A block relative to the number-averaged size and the polydisperse index is $\text{PDI}_A = (k+1)/k$. The numerics are performed with the efficient algorithm introduced earlier [10], where the diffusion equation is solved using the spectral method [28] and integrations over the molecular-weight distribution are evaluated using Gaussian quadrature [15]. We use up to $M = 2000$ symmetrized basis functions and quadratures of order $n_g = 300$ so as to ensure that numerical inaccuracies are negligible on the scale of our plots. The self-consistent field equations are generally solved using

the Broyden method when $M \lesssim 100$ and Anderson mixing when $M \gtrsim 100$, which keeps the computational cost of the calculation relatively modest [29].

We start by comparing the phase diagrams of AB diblock and BAB triblock copolymer melts plotted in terms of A-block volume fraction, f_A , and segregation, χN , with the polydispersity index of the A block set to $\text{PDI}_A = 1.5$. As expected, the order-order transitions (OOTs) are shifted towards larger f_A compared to the monodisperse case examined earlier (see ref. [19]), and indeed the effect is more significant for the triblocks as suggested by the experiments [18]. As mentioned in the Introduction, SCFT does not predict the correct shift in the order-disorder transition (ODT) because it fails to account for packing frustration in the disordered phase. Nevertheless, fig. 2 illustrates that the tendency of the higher molecular-weight molecules to microphase separate, which acts to decrease $(\chi N)_{\text{ODT}}$ relative to that of the monodisperse melts (dashed curves), is quantitatively similar for both the diblock and triblock architectures.

There are also some other intriguing features in the phase diagrams, apart from the shifts in the phase boundaries. As discovered earlier for diblocks [11], the usual bcc spherical (S) phase gives way to the close-packed spherical (S_{cp}) phase; however, this is much more pronounced in the triblock system. What was not realized in the earlier study was that the spherical micelles reorder into an A15 arrangement once their coronas become thin relative to their cores (on left side of the diagrams), which has incidentally been predicted [19, 30, 31] and observed [32] in other systems where the spherical phase is shifted towards high minority-component compositions. It is also intriguing that on the right side of both phase diagrams the stability regions of the complex Fddd (O^{70}) phase have expanded considerably relative to those of monodisperse melts [19].

To better quantify the enhanced shift of the OOTs for triblocks relative to diblocks, fig. 3 plots both of their phase diagrams as a function of composition, f_A , and polydispersity, PDI_A , at a fixed segregation of $\chi N = 30$. As we can see, the triblock OOTs are already shifted relative to the diblock ones even for monodisperse melts; the center of the lamellar region occurs at $f_A = 0.518$ for the triblocks as compared to $f_A = 0.5$ for the diblocks. Nevertheless, polydispersity increases this difference. By $\text{PDI}_A = 2.0$, the center of the lamellar region occurs at $f_A = 0.665$ for triblocks as compared to $f_A = 0.613$ for diblocks, resulting in a difference of $\Delta f_A = 0.052$ which is three times the $\Delta f_A = 0.018$ for monodisperse melts. In fact, this SCFT prediction for the polydisperse triblock copolymer melts agrees perfectly with the location, $f_A = (0.57 + 0.75)/2 = 0.66$, reported by the experiments of Widin *et al.* [18]. Furthermore, the complex-phase window occurs near $f_A \approx 0.5$ for the polydisperse triblocks in agreement with their earlier experiments [16], whereas the polydisperse diblocks still form a lamellar phase at symmetric compositions.

Interestingly, the perforated-lamellar (PL) phase becomes stable for triblock melts on the right side of the

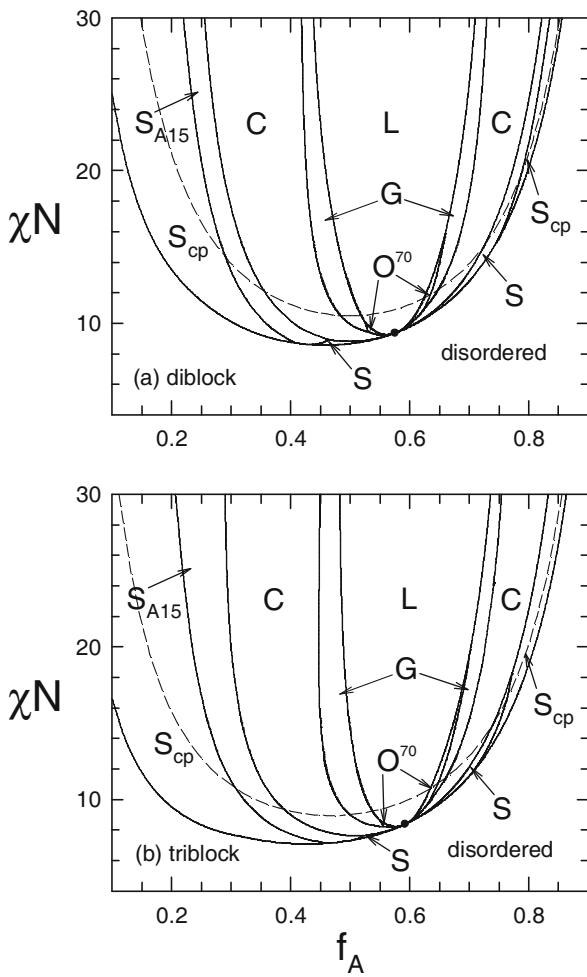


Fig. 2. Phase diagrams for melts of (a) AB diblock and (b) BAB triblock copolymer with polydisperse A blocks ($PDI_A = 1.5$) and monodisperse B blocks ($PDI_B = 1.0$) plotted as a function of A-block composition, f_A , and segregation, χN , where N is the number-averaged polymerization index of a complete diblock or half a triblock. The ordered phases are lamellar (L), cylindrical (C), bcc spherical (S), closed-packed spherical (S_{cp}), A15 spherical (S_{A15}), gyroid (G), and Fddd (O^{70}). Two-phase coexistence regions are ignored, and the mean-field critical points are marked by solid dots. The dashed curves denote the ODTs for monodisperse melts.

phase diagram (fig. 3b), where the thinner monodisperse lamellae develop perforations through which the thicker polydisperse domains are connected. The PL phase is nearly stable in the same region of the diblock phase diagram. Incidentally, experiments by Listak *et al.* [7] did observe PL in polydisperse diblocks, but oddly on the other side of the phase diagram at a surprisingly low composition of $f_A = 0.35$ considering their estimates of $PDI_A = 1.8$ and $PDI_B = 1.1$; they did, however, report that their samples could have been affected by residual macroinitiator and that their polydisperse blocks were not well represented by the Schulz-Zimm distribution. One other notable feature of our triblock phase diagram is

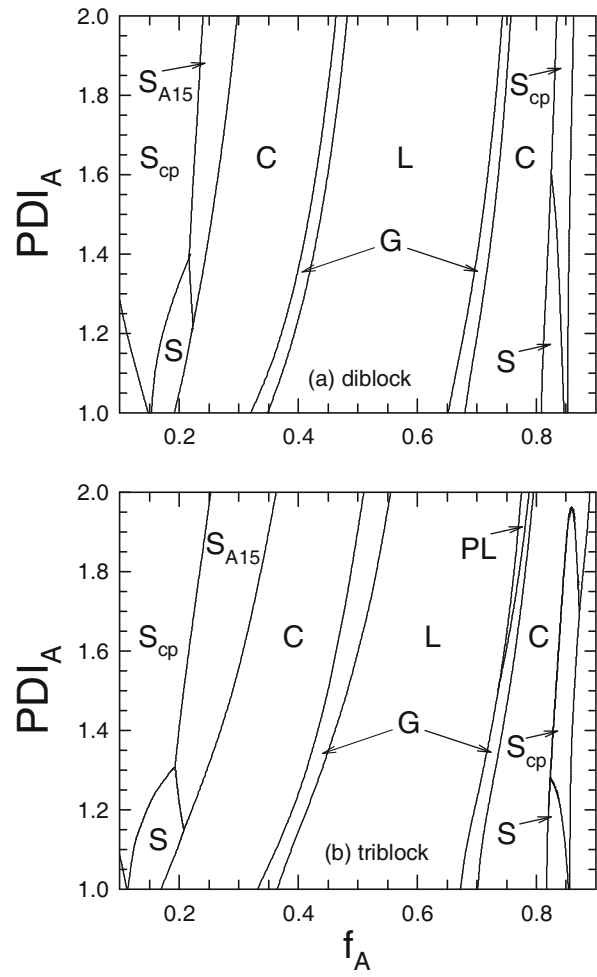


Fig. 3. Similar diagrams to those of fig. 2, but plotted as a function of A-block composition, f_A , and A-block polydispersity, PDI_A , at a fixed segregation of $\chi N = 30$. Note that an additional ordered phase of perforated-lamellae (PL) becomes stable in the triblock system.

that the spherical phase vanishes on the right side at $PDI_A > 1.96$ for some unknown reason; consequently the cylinder phase extends to the ODT.

In addition to the pronounced shift in the OOTs, the experiments on polydisperse triblocks [17,18] also reported a dramatic expansion in domain size. Our SCFT calculations do generally predict larger domains for triblocks than for the corresponding diblocks, but this has little to do with polydispersity. Figure 4 compares the dilation of the lamellar period, D , due to polydispersity, PDI_A , for compositionally symmetric triblocks (solid curves) and diblocks (dashed curves). Although polydispersity tends to have a greater effect on the triblock copolymer melts, the difference is very slight. In reality, most of the difference in domain size is already present for monodisperse melts [33], as illustrated in the inset where the lamellar period, D_0 , is plotted for $PDI_A = 1.0$.

According to strong-segregation theory (SST), the lamellar period of both monodisperse systems is given

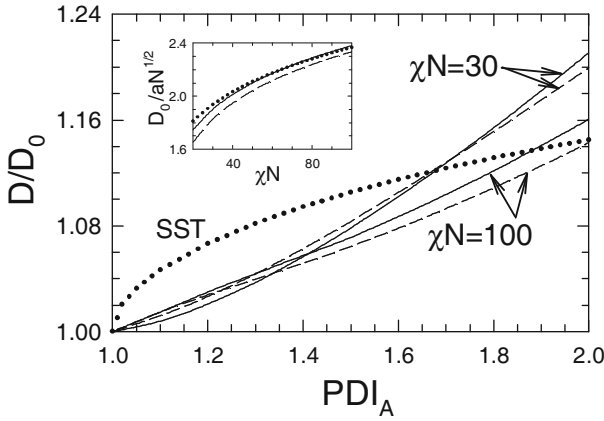


Fig. 4. Lamellar period, D , relative to that of a monodisperse melt, D_0 , plotted as a function of polydispersity, PDI_A , at symmetric composition, $f_A = 0.5$, and two different degrees of segregation, χN . The inset shows D_0 as a function of χN . Solid and dash curves denote results for triblock and diblock melts, respectively, while the dotted curves denote the $\chi N \rightarrow \infty$ limits from eqs. (2) and (3).

by [21]

$$D_0 = 2 \left(\frac{8\chi N}{3\pi^4} \right)^{1/6} aN^{1/2}, \quad (2)$$

and indeed this prediction (dotted curve) agrees reasonably well with our SCFT calculations in the inset of fig. 4. Likewise, SST predicts a dilation [10]

$$\frac{D}{D_0} = \frac{1}{[f_A S_A + 1 - f_A]^{1/3}}, \quad (3)$$

with an identical dependence on the molecular-weight distribution

$$S_A = \int_0^\infty \left[1 - \int_0^\sigma p_\alpha(\sigma') d\sigma' \right]^3 d\sigma, \quad (4)$$

for both architectures. Although this SST prediction (dotted curve) is not a particularly good approximation of our SCFT results in fig. 4, it does corroborate our conclusion that polydispersity has a quantitatively similar effect on the domain sizes of both the diblock and triblock copolymer melts.

Mahanthappa *et al.* [17,18] suggested that a contributing factor to the enhanced polydispersity effects in their BAB triblock copolymer melts could be the *pull-out* of short A blocks from their domains, swelling the B-rich regions and producing a shift in the OOTs consistent with the addition of B-type homopolymer [34,35]. Figure 5 examines the swelling in the lamellar phase as a function of polydispersity by plotting the volume of the B-rich domain, V_B , relative to the expected volume based on the composition, $(1 - f_A)V$. Note that we define the internal interfaces of the morphology as the surfaces of equal A and B concentration (*i.e.*, $\phi_A(\mathbf{r}) = \phi_B(\mathbf{r})$). Although there is some swelling of the B-rich domains, it is too small to

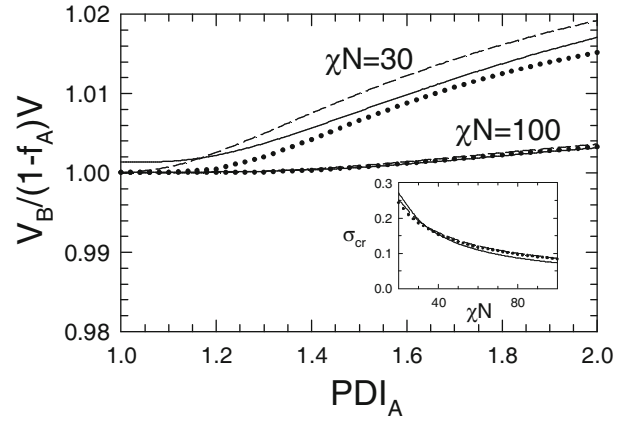


Fig. 5. Volume of the B-rich domain, V_B , relative to the total volume occupied by B segments, $(1 - f_A)V$, plotted as a function of polydispersity, PDI_A , at symmetric composition, $f_A = 0.5$, and two different degrees of segregation, χN . The inset shows the critical size, σ_{cr} , for chain *pull-out* as a function of χN . Solid and dash curves denote results for triblock and diblock melts, respectively, while the dotted curves denote the $\chi N \rightarrow \infty$ limits from eqs. (5) and (6).

have a significant effect. In any case, the swelling cannot account for the dramatic behavior observed in the triblock experiments, given that it is just as large, or in fact slightly larger, for diblock copolymer melts.

SST again accounts for the similar behavior of the diblock and triblock copolymer melts. The dotted curve in fig. 5 plots the relative swelling of the B-rich domains

$$\frac{V_B}{(1 - f_A)V} = 1 + \frac{f_A}{1 - f_A} \int_0^{\sigma_{\text{cr}}} \sigma p(\sigma) d\sigma, \quad (5)$$

assuming that all A blocks below a critical size, σ_{cr} , are pulled into the B-rich domains. In a previous SST-based calculation for the lamellar phase of a diblock copolymer melt [11], the critical size was derived to be

$$\sigma_{\text{cr}} = \frac{1}{\chi N f_A} \left[\frac{2aN^{1/2}}{D} \sqrt{\frac{\chi N}{6}} + \frac{\pi^2(1 - f_A)D^2}{32a^2N} \right], \quad (6)$$

which is plotted in the inset of fig. 5 for $\text{PDI}_A = 1.0$. Note that σ_{cr} has a small dependence on PDI_A , because of the dilation in D . The expression in eq. (6) is obtained by balancing the enthalpic cost of pulling an A block into a B-rich domain with the entropic gain of relaxing the B block to which it is attached. Although the A block of a BAB triblock is twice as large, it is attached to two B blocks and thus the same expression (6) also applies to triblocks. In SCFT, σ_{cr} can be defined as the relative size of an A block below which its segments are more likely to be found in a B-rich domain rather than an A-rich domain [10]. Using this definition, the SCFT predictions of σ_{cr} for triblocks (solid curves) and diblocks (dashed curves) are virtually identical and in excellent agreement with eq. (6). Since the enhanced polydispersity effects in

triblock copolymer melts cannot be attributed to the pull-out of short A blocks from their domains, they must instead be due to an entropic difference in the A-rich domains regarding how polydispersity affects the packing of middle blocks *versus* end blocks.

3 Discussion

Melts of symmetric triblock copolymer should behave quantitatively similar to melts of diblock copolymer, provided that the polymers are sufficiently flexible that they can be modeled as Gaussian chains. This follows from the strong-segregation theory (SST) of Semenov [21], which says that a block constrained by both ends to an internal interface is unaffected by snipping it in half. The implication is that complex block-copolymer architectures are governed by their constituent units [19, 36–38], and in particular symmetric BAB triblocks of polymerization $2N$ behave the same as AB diblocks of polymerization N [39]. This equivalence is exact in the strong-segregation limit, which implies that the OOTs in figs. 2a and b must become identical as $\chi N \rightarrow \infty$. It is also why the SST predictions in eqs. (2), (3) and (6) are the same for both architectures.

Of course, there will be some differences in behavior at finite degrees of segregation, as evident by previous SCFT calculations [33] on monodisperse triblock and diblock copolymer melts. Indeed, the finite-segregation corrections to SST [22, 40] will differ for the two architectures. The most obvious difference will involve the free-energy correction per chain due to the entropy of free ends, which takes the form

$$\frac{\Delta F_{\text{ends}}}{nk_B T} = -\ln(L) + k_1 + k_2 L^{-2/3} + k_3 L^{-4/3} + \dots, \quad (7)$$

where L is the domain thickness. For extraordinarily large χN , the logarithmic term, which favors large L , dominates. However, for realistic values of χN , the negative powers of L become more important. As it happens, their coefficients (*i.e.*, k_2 and k_3) are generally negative and therefore they favor small L . It follows that triblocks should have slightly larger domains than diblocks, since there are no chain ends in their middle-block domains [41]. The relative corrections to the different morphologies is a more subtle affair, but the asymmetry in the monodisperse triblock phase diagram [33] implies that end segments are favored on the outside of the interfacial curvature. We suggest that these chain-end effects, which presumably account for the small differences in the domain sizes and OOTs between monodisperse triblocks and diblocks, are simply enhanced by polydispersity.

As eluded to earlier, the position of the lamellar region, $0.57 \lesssim f_A \lesssim 0.75$, in the experiment of Widin *et al.* [18] agrees remarkably well with the interval, $0.555 \leq f_A \leq 0.775$, predicted by SCFT for $\text{PDI}_A = 2.0$ in fig. 3b. However, this neglects the fact that the experimental system had a small polydispersity of $\text{PDI}_B \approx 1.2$

in the end blocks as well as a significant degree of conformational asymmetry, $a_A/a_B = 1.3$ [42]. Based on the typical shifts observed in fig. 3, we would expect this level of B-block polydispersity to move the lamellar region to the left by $\Delta f_A \approx -0.05$. As it happens, previous SCFT calculations [33] on monodisperse triblocks investigated this particular level of conformational asymmetry and found that it shifts the lamellar region to the right by $\Delta f_A \approx 0.05$ at $\chi N = 30$. Thus these two corrections to the OOTs should approximately cancel, preserving the good agreement between SCFT and experiment. On the other hand, both B-block polydispersity and conformational asymmetry contribute to a dilation of the domains, which would naturally bring the SCFT predictions into better agreement with experiments. In fact, according to previous calculations on diblocks [10], the dilation is enhanced considerably when there is polydispersity in both domains. Still, this is not enough, even when combined with the conformational asymmetry, to account for the dramatic dilations reported by the experiments [16–18].

In some instances, particularly near phase boundaries, a melt can lower its free energy by fractionating its molecular-weight distribution into two coexisting phases. A previous SCFT calculation [11] for diblock copolymer melts showed that with sufficient polydispersity, the complex-phase windows are gradually replaced by L+C coexistence. However, this macrophase separation is a far slower process than microphase separation. The later only requires a local rearrangement of A and B blocks, whereas the former requires the macroscopic transport of the more symmetric molecules to a lamellar region while the more asymmetric molecules migrate to a cylindrical region. Our present calculation simply assumes that the time scale of the experiment is insufficient for macrophase separation to occur, which is a sensible expectation for high molecular-weight systems [43]. Indeed the experiments in refs. [16, 18] revealed no evidence of two-phase coexistence. There would still be a tendency for the complex phases (*i.e.*, G, O⁷⁰ and PL) to macrophase separate into C+L, and this is likely why the experiments observed disordered bicontinuous morphologies in the complex-phase channels. Naturally, our assumption breaks down for the faster dynamics of small molecules, and indeed L+C coexistence has been reported for lower molecular-weight systems [17, 44]. Nevertheless, the L+C coexistence should simply replace the complex-phase channel without altering its location, and so our phase diagrams would still be relevant.

It is well understood that polydispersity relieves the packing frustration caused by difficult-to-fill regions in the morphology, which occur when there are large variations in domain thickness [25, 45]. In the polydisperse domains, these regions can be filled by the higher molecular-weight blocks of the distribution, and in the monodisperse domains, they can be filled by the polymers that pull-out from the interface. Given that cylindrical and spherical micelles self-assemble into regular arrays so as to reduce packing frustration in the matrix domain, it follows that polydispersity should reduce the long-range order in these phases.

Indeed, the experiments in refs. [17, 18] only observed disordered cylinders on the large- f_A side of the phase diagram, where the matrix is polydisperse.

This suppression of ordering by a reduction in packing frustration presumably shifts the ODT to larger χN , counteracting the downward shift in fig. 2 caused by the enhanced tendency of the higher molecular-weight chains to order. Near the ODT, even the disordered phase microphase separates, but into irregularly shaped domains with high levels of packing frustration. Because its packing frustration is much greater than that of an ordered phase, the relative stability of the disordered phase will be enhanced by polydispersity [13, 14]. SCFT misses this effect because it treats the disordered phase as a homogeneous mixture of A and B segments, in which there is no packing frustration. In any case, this packing-related effect should apply equally to triblocks as it does to diblocks, and thus it is difficult to understand why experiments [16, 18] find such low values of $(\chi N)_{\text{ODT}}$ for polydisperse triblock copolymer melts.

Although SCFT nicely accounts for the shift in the OOTs reported by Mahanthappa and coworkers, the dramatic increase in their domain sizes and stability of the ordered phases remains a mystery. Perhaps these effects are not entirely due to the triblock architecture. Indeed there has been a couple reported cases [46, 47] where experiments observed unexpectedly large dilations in polydisperse diblock copolymer melts. It was suggested that the dilation occurs because the penalty for swollen domains is reduced by the occurrence of chain pullout. This claim was supported by a SST-based calculation [46], and indeed our SCFT calculation predicts the same albeit to a much lesser extent. Nevertheless, this effect alone is insufficient to explain how the morphology selects a single dilated domain size for the lamellar phase, rather than a wide spectrum of domain sizes resulting in a disordered phase.

One issue yet to be considered is the detailed shape of the molecular-weight distribution. Like most calculations, we use the Schulz-Zimm distribution because of its simple functional form, eq. (1), that bridges between the most-probable distribution ($k = 1$) and monodisperse blocks ($k \rightarrow \infty$). However, the polydispersity distribution of some experiments may have a very different shape (*e.g.*, skewness [7]) to that of the Schulz-Zimm distribution, and this could be important at large PDI. In fact, a previous SCFT calculation [48] for a more realistic distribution with equivalent PDI predicted a significant enhancement in domain size without causing much of an effect on the position of the phase boundaries between lamellae and cylinders (and thus presumably on the location of the complex phase channels). In that case, the more realistic distribution had a higher fraction of molecules with $\sigma < \sigma_{\text{cr}}$, which presumably caused a greater swelling of the monodisperse domains. This is just a single example, but it does demonstrate that characterizing a molecular-weight distribution by PDI alone is not entirely sufficient when the polydispersity is large.

4 Summary

This study has addressed the issue of whether or not block copolymer melts are affected differently by polydispersity in middle blocks *versus* end blocks. Using self-consistent field theory (SCFT), we compared BAB triblocks and AB diblocks with number-averaged polymerizations of $2N$ and N , respectively, where the A blocks are polydisperse and the B blocks are monodisperse. In both cases, polydispersity causes a dilation of the domains, shifts the order-order transitions (OOTs) to higher f_A , and moves the order-disorder transition (ODT) to lower χN . Note that SCFT omits a packing-related effect [13, 14] that counteracts the downward shift in $(\chi N)_{\text{ODT}}$, which is presumably similar for both architectures. Polydispersity also causes spherical micelles to reorder into an A15 arrangement (S_{A15}) on the small- f_A side of the phase diagram, and it helps stabilize the complex Fddd (O^{70}) and perforated-lamellar (PL) phases on the large- f_A side.

Strong-stretching theory (SST) predicts quantitatively identical behavior for the triblock and diblock systems, but recent experiments [16–18] from the group of Mahanthappa suggest that the polydispersity effects are dramatically enhanced in the triblock system. Our SCFT calculations do, in fact, predict larger shifts in the OOTs for triblocks than diblocks, which we attribute to the absence of chain ends and their associated entropy in the middle-block domains. While SCFT does predict a slightly enhanced dilation of the domains for triblocks, it is nowhere near the amount suggested by the experiments. Furthermore, our calculations indicate that polydispersity should have similar effects on the ODTs of both systems. Thus it appears that the enhanced effects observed by the experiments are not entirely due to the triblock architecture. Experiments on matched triblock and diblock systems could help establish whether or not this is the case.

It should be noted that our calculations are specific to the Schulz-Zimm molecular-weight distribution [26, 27], which may not be a good representation of the experimental distribution. It is conceivable that the dramatic dilation of the domains and the enhanced stability of ordered phases may have more to do with the detailed shape of the distribution than the triblock architecture. This highlights the need for further SCFT calculations to investigate how the behavior of polydisperse block copolymer melts is affected by the skewness of the molecular-weight distribution.

We are grateful to Mahesh Mahanthappa for useful discussions and to the EPSRC for funding this work.

References

1. M.A. Hillmyer, J. Polym. Sci. Part B **45**, 3249 (2007).
2. N.A. Lynd, A.J. Meuler, M.A. Hillmyer, Prog. Polym. Sci. **33**, 875 (2008).
3. D. Bendejacq, V. Ponsinet, M. Joanicot, Y.-L. Loo, R.A. Register, Macromolecules **35**, 6645 (2002).

4. N.A. Lynd, B.D. Hamilton, M.A. Hillmyer, *J. Polym. Sci. Part B* **45**, 3386 (2007).
5. N.A. Lynd, M.A. Hillmyer, *Macromolecules* **38**, 8803 (2005).
6. N.A. Lynd, M.A. Hillmyer, *Macromolecules* **40**, 8050 (2007).
7. J. Listak, W. Jakubowski, L. Mueller, A. Plichta, K. Matyjaszewski, M.R. Bockstaller, *Macromolecules* **41**, 5919 (2008).
8. A.-V. Ruzette, S. Tencé-Girault, L. Leibler, F. Chauvin, D. Bertin, O. Guerret, P. Gérard, *Macromolecules* **39**, 5804 (2006).
9. D.M. Cooke, A.-C. Shi, *Macromolecules* **39**, 6661 (2006).
10. M.W. Matsen, *Eur. Phys. J. E* **21**, 199 (2006).
11. M.W. Matsen, *Phys. Rev. Lett.* **99**, 148304 (2007).
12. S.T. Milner, T.A. Witten, M.E. Cates, *Macromolecules* **22**, 853 (1989).
13. T.M. Beardsley, M.W. Matsen, *Eur. Phys. J. E* **27**, 323 (2008).
14. T.M. Beardsley, M.W. Matsen, *Macromolecules* **44**, 6209 (2011).
15. S.W. Sides, G.H. Fredrickson, *J. Chem. Phys.* **121**, 4974 (2004).
16. J.M. Widin, A.K. Schmitt, K. Im, A.L. Schmitt, M.K. Mahanthappa, *Macromolecules* **43**, 7913 (2010).
17. A.L. Schmitt, M.K. Mahanthappa, *Soft Matter* **8**, 2294 (2012).
18. J.M. Widin, A.K. Schmitt, A.L. Schmitt, K. Im, M.K. Mahanthappa, *J. Am. Chem. Soc.* **134**, 3834 (2012).
19. M.W. Matsen, *Macromolecules* **45**, 2161 (2012).
20. E. Helfand, *J. Chem. Phys.* **62**, 999 (1975).
21. A.N. Semenov, *Sov. Phys. JETP* **61**, 733 (1985).
22. M.W. Matsen, *Eur. Phys. J. E* **33**, 297 (2010).
23. M.W. Matsen, in *Soft Matter*, Vol. 1: *Polymer Melts and Mixtures*, edited by G. Gompper, M. Schick (Wiley-VCH, Weinheim, 2006).
24. G.H. Fredrickson, *The Equilibrium Theory of Inhomogeneous Polymers* (Oxford University Press, New York, 2006).
25. M.W. Matsen, *J. Phys.: Condens. Matter* **14**, R21 (2012).
26. G.V.Z. Schulz, *Z. Phys. Chem. (Munich)* **B43**, 25 (1939).
27. B.H. Zimm, *J. Chem. Phys.* **16**, 1099 (1948).
28. M.W. Matsen, M. Schick, *Phys. Rev. Lett.* **72**, 2660 (1994).
29. M.W. Matsen, *Eur. Phys. J. E* **30**, 361 (2009).
30. G.M. Grason, R.D. Kamien, *Phys. Rev. Lett.* **91**, 7371 (2004).
31. G.M. Grason, B.A. DiDonna, R.D. Kamien, *Phys. Rev. Lett.* **91**, 058304 (2003).
32. B.-K. Cho, A. Jain, S.M. Gruner, U. Wiesner, *Science* **305**, 1598 (2004).
33. M.W. Matsen, R.B. Thompson, *J. Chem. Phys.* **111**, 7139 (1999).
34. M.W. Matsen, *Macromolecules* **28**, 5765 (1995).
35. M.W. Matsen, *Macromolecules* **36**, 9647 (2003).
36. M. Xenidou, F.L. Beyer, N. Hadjichristidis, S.P. Gido, N. Bech Tan, *Macromolecules* **31**, 7659 (1998).
37. C. Lee, S.P. Gido, Y. Poulos, N. Hadjichristidis, N. Bech Tan, S.F. Trevino, J.W. Mayes, *Polymer* **39**, 4631 (1998).
38. F. Beyer, S.P. Gido, C. Bushchi, H. Iatrou, D. Uhrig, J.W. Mayes, M. Chang, B.A. Garetz, N. Balsara, N. Bech Tan, N. Hadjichristidis, *Macromolecules* **33**, 2039 (2000).
39. S.-M. Mai, W. Mingvanish, S.C. Turner, C. Chaibundit, J.P.A. Fairclough, F. Heatley, M.W. Matsen, A.J. Ryan, C. Booth, *Macromolecules* **33**, 5124 (2000).
40. A.E. Likhtman, A.N. Semenov, *Europhys. Lett.* **51**, 307 (2000).
41. Middle blocks have a similar correction to eq. (7) for the entropy of their center segments, but it is roughly half the size. This is because each center segment becomes two ends when a middle block is snipped in half.
42. L.J. Fetters, D.J. Lohse, D. Richter, T.A. Witten, A. Zirkel, *Macromolecules* **27**, 4639 (1994).
43. P.M. Lipic, F.S. Bates, M.W. Matsen, *J. Polym. Sci., Part B* **37**, 2229 (1999).
44. L.M. Pitet, M.A. Hillmyer, *Macromolecules* **42**, 3674 (2009).
45. M.W. Matsen, F.S. Bates, *Macromolecules* **29**, 7641 (1996).
46. P.D. Hustad, G.R. Marchand, E.I. Garcia-Meitin, P.L. Roberts, J.D. Weinhold, *Macromolecules* **42**, 3788 (2009).
47. S. Li, R.A. Register, B.G. Landes, P.D. Hustad, J.D. Weinhold, *Macromolecules* **43**, 4761 (2010).
48. N.A. Lynd, M.A. Hillmyer, M.W. Matsen, *Macromolecules* **41**, 4531 (2008).